Vulnerability of Coral Reefs to Bioerosion From Land-Based Sources of Pollution

Nancy G. Prouty[1] iD **, Anne Cohen[2]** iD **, Kimberly K. Yates[3], Curt D. Storlazzi[1]** iD **, Peter W. Swarzenski[1,4], and Darla White[5]**

[1]U.S. Geological Survey, Pacific Coastal and Marine Science Center, Santa Cruz, CA, USA, [2]Department of Geology and Geophysics, Woods Hole Oceanographic Institution, Woods Hole, MA, USA, [3]U.S. Geological Survey, St. Petersburg Coastal and Marine Science Center, St. Petersburg, FL, USA, [4]International Atomic Energy Agency, Principality of Monaco, Monaco, [5]Division of Aquatic Resources, Department of Land and Natural Resources, Maui, HI, USA

Abstract Ocean acidification (OA), the gradual decline in ocean pH and $[CO_3^{2-}]$ caused by rising levels of atmospheric CO_2, poses a significant threat to coral reef ecosystems, depressing rates of calcium carbonate ($CaCO_3$) production, and enhancing rates of bioerosion and dissolution. As ocean pH and $[CO_3^{2-}]$ decline globally, there is increasing emphasis on managing local stressors that can exacerbate the vulnerability of coral reefs to the effects of OA. We show that sustained, nutrient rich, lower pH submarine groundwater discharging onto nearshore coral reefs off west Maui lowers the pH of seawater and exposes corals to nitrate concentrations 50 times higher than ambient. Rates of coral calcification are substantially decreased, and rates of bioerosion are orders of magnitude higher than those observed in coral cores collected in the Pacific under equivalent low pH conditions but living in oligotrophic waters. Heavier coral nitrogen isotope (δ^{15}N) values pinpoint not only site-specific eutrophication, but also a sewage nitrogen source enriched in ^{15}N. Our results show that eutrophication of reef seawater by land-based sources of pollution can magnify the effects of OA through nutrient driven-bioerosion. These conditions could contribute to the collapse of coastal coral reef ecosystems sooner than current projections predict based only on ocean acidification.

Plain Language Summary We show that sustained, nutrient rich, lower pH submarine groundwater discharging onto nearshore coral reefs off west Maui lowers the pH of seawater and exposes corals to nitrate concentrations 50 times higher than ambient. Rates of coral calcification are substantially decreased, and rates of bioerosion are orders of magnitude higher than those observed in coral cores collected in the Pacific. With many of Maui's coral reefs in significant decline reducing any stressors at a local scale is important to sustaining future coral reef ecosystems and planning for resiliency.

1. Introduction

Coral reefs occupy less than 1% of the world's seafloor yet support hundreds of thousands of animal and plant species (Reaka-Kudla, 1987), sustain the livelihoods of hundreds of millions of people around the world, and protect thousands of kilometers of coastline from coastal hazards (Ferrario et al., 2014; Hughes et al., 2003). Yet coral reefs are facing increasing stress from global climate change, such as increasing temperatures, sea levels, and ocean acidification (OA), combined with local stressors from overfishing, sedimentation, and land-based sources of pollution including coastal acidification (Knowlton & Jackson, 2008). As discussed in early work on carbonate budgets by Stearn et al. (1977), and Scoffin et al. (1980), the carbonate accretion of coral reefs depends on two overarching processes: production of calcium carbonate ($CaCO_3$) skeletons by plants and animals on the reef and cementation of sand and rubble, and $CaCO_3$ breakdown and removal that occurs through bioerosion, dissolution, and offshore transport (e.g., Glynn & Manzello, 2015; Perry et al., 2013). Accretion of $CaCO_3$ must exceed removal for modern reefs to be in a state of net growth. However, any factor facilitating the decrease of carbonate production could tip this balance, causing reefs to shift to a state of net loss. There is now strong evidence that calcification rates tend to decrease, and bioerosion and dissolution rates tend to increase with declining seawater pH and $[CO_3^{2-}]$ (Anthony et al., 2008; Enochs et al., 2016; Hughes et al., 2007). Under elevated aqueous pCO_2 (750 μatm) treatments,

biogenic dissolution by euendolith (microborers) communities were found to yield a dissolution rate of 39 g $CaCO_3$ m^{-2} mo^{-1} (46.8 mg cm^{-2} yr^{-1}); Tribollet et al., 2009). This is consistent with field observations from Oahu where bioerosion rates were highly sensitive to ocean pH (Silbiger et al., 2014, 2016). Nutrient loading can also accelerate bioerosion rates (Carreiro-Silva et al., 2005, 2009; Holmes et al., 2000), as revealed at sites that were exposed to inorganic nutrient loading in the absence of macrograzers having bioerosion rates enriched by a factor of 10 (Carreiro-Silva et al., 2005). Therefore, past studies indicate that both OA and nutrient loading separately can increase bioerosion rates. However, there is now compelling evidence that sensitivity to bioerosion is much magnified under multiple stressors, including stressors from nutrient and sediment loading, along with overfishing (Ban et al., 2014; DeCarlo et al., 2015; Vega Thurber et al., 2014). Recently, DeCarlo et al. (2015) found macrobioerosion rates 10 times greater under high-nutrient conditions. Bioerosion rates of corals collected from naturally low pH environments were 10 times faster under nutrient-rich (eutrophic) conditions compared with nutrient poor (oligotrophic) conditions. Although this observation was made on pristine, unpolluted reef systems, it highlights the potential dangers of nutrients to magnifying OA effects. This is of particular concern to coral reefs adjacent to densely inhabited shore-lines, where nutrient fluxes can be high due to upstream fertilized, agricultural lands, treated wastewater injection, and leakage from leech field and septic systems close to shore.

Situated in the North Pacific Subtropical Gyre, the coral reef islands of Hawaii occupy a tropical, oligotrophic region with naturally occurring, low-nutrient concentrations. On the Hawaiian island of Maui, however, anthropogenic nutrient loading to coastal waters via sustained submarine groundwater discharge (SGD) has been well documented (Amato et al., 2016; Bishop et al., 2015; Dailer et al., 2010, 2012; Fackrell et al., 2016). SGD consists of both terrestrial groundwater and recirculated seawater that is influenced by tides and waves (Dimova et al., 2012). In Hawaii, where rivers are not abundant and permeability is high within the basaltic bedrock, SGD is an important water-borne transport vector for nutrients into the coastal ocean (Amato et al., 2016; Bienfang, 1980; Fackrell et al., 2016; Hunt & Rosa, 2009; Nelson et al., 2015; Parsons et al., 2008; Peterson et al., 2009; Swarzenski et al., 2012, 2016). As a result, SGD can impact the structure of marine biotic communities by delivering elevated nutrient loads that may lead to eutrophication, harmful algal blooms (Anderson et al., 2002), decreased coral abundance and diversity, and increased macroalgal abun-dance (Fabricius, 2005; Lapointe et al., 2005), as well as low pH water that can cause coastal acidification (Wang et al., 2014). Eutrophication, for example, from nitrogen and phosphorous pollution of land-based sources, such as septic leachate and fertilizers, can alter ecosystem function and structure by shifting reefs from being dominated by corals to being dominated by algae (Andrefouet et al., 2002; Howarth et al., 2000; Hughes et al., 2007) and increasing the vulnerability of reefs to coral disease (Bruno et al., 2003; Redding et al., 2013).

"Dead zones," areas of clustered patches of variable degrees of degradation with discrete coral cover loss of nearly 100% have been observed for decades (Ross et al., 2012; Wiltse, 1996) along the shallow coral reef at Kahekili in Kaanapali, west Maui, Hawaii, USA (Figure 1). This area has a long history of macroalgal blooms (Smith et al., 2005) and a decrease in herbivorous fishes attributed to overfishing (Williams et al., 2016). As a result, there has been a shift over the past decades in benthic cover from abundant corals to turf-algae or macroalgae (Cochran et al., 2014). Currently, only 51% of the hardbottom at Kahekili is covered with at least 10% live coral (Cochran et al., 2014). Excessive algae growth has been a concern since the late 1980s, with potential links to input of nutrient-rich water via wastewater injection wells (Dailer et al., 2010, 2012). Fluo-rescent dye tracer studies now confirm that there is a direct hydrologic link between the nearby Lahaina Wastewater Reclamation Facility (LWRF) and SGD, where treated wastewater is injected into groundwater that then flows toward the coast to emerge through a network of small seeps and vents (Glenn et al., 2013; Swarzenski et al., 2016). Changes in coastal water quality observed off west Maui can ultimately impact the balance between reef accretion and bioerosion, with reef degradation occurring through both the biologi-cal breakdown of the skeleton from microborers (e.g., alga and bacteria) and macroborers (e.g., bivalves and sponges; Osorno et al., 2005) via mechanical and chemical bioerosion (see reviews by Schönberg et al., 2017; Tribollet & Golubic, 2011) as well as dissolution of $CaCO_3$ due to changes in the aragonite saturation state (Ω_{arag}) from both natural (Crook et al., 2012, 2013; Shamberger et al., 2014; Silbiger et al., 2014) and anthropogenic activities (Fabricius et al., 2011; Hoegh-Guldberg et al., 2007; Kleypas et al., 1999).

We investigated the influence of SGD on reef biogeochemistry and growth of massive reef-building corals on a shallow reef at Kahekili in Kaanapali, west Maui, Hawaii, USA (Figure 1), where the
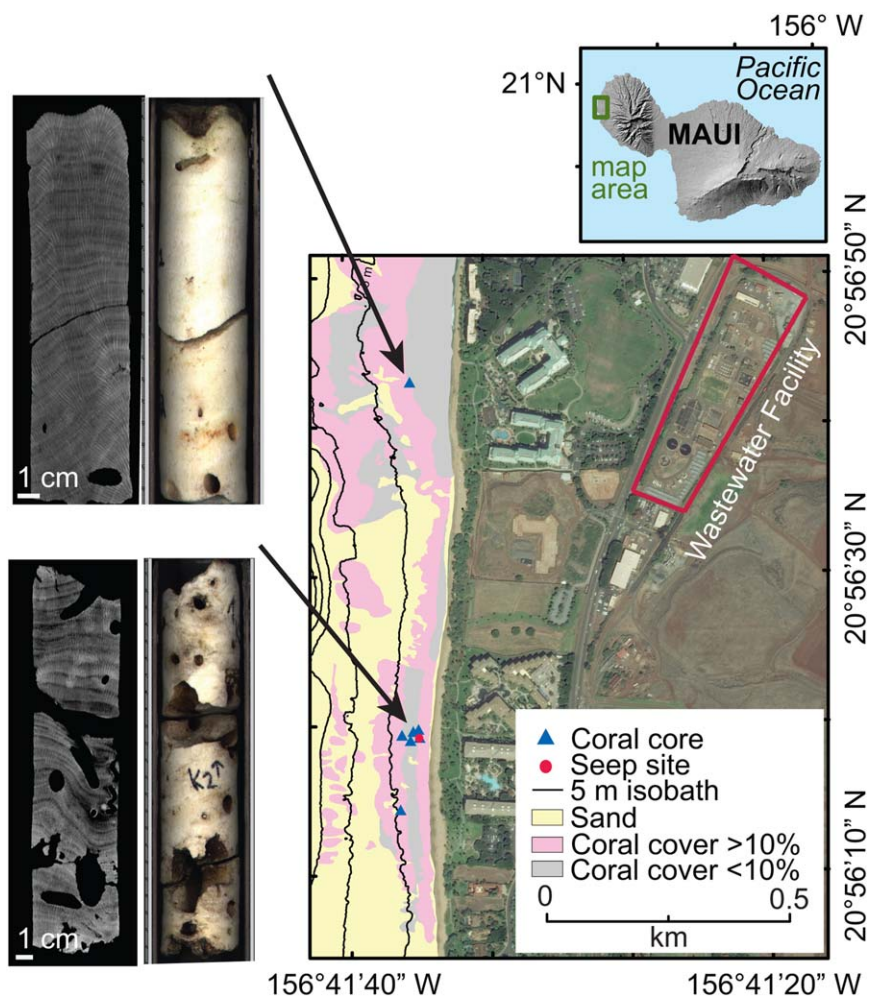
Figure 1. Location map of the island of Maui, Hawaii, USA, and the study area at Kahekili along west Maui. Bathymetric map (5 m contours) of study area showing coral coring locations and seawater sampling sites (blue triangles) along Kahekili, primary seep site (red circle), superimposed on distribution of percent coral cover versus sand. Computerized tomography (CT) images and respective photographs of coral cores collected at the primary seep site and north of the primary seep site, approximately 780 m north of the primary seep cluster at Kahekili.

existence of numerous low salinity seeps provide a direct vector for low pH, nutrient-rich groundwater onto the reef (Glenn et al., 2013; Swarzenski et al., 2016). Sampling to characterize seawater chemistry at the primary seep site and in adjacent coastal waters was conducted in September 2014 and March 2016. Water samples were collected and analyzed for salinity, dissolved inorganic nutrients, and seawater carbonate system parameters (pH (total scale), total alkalinity (TA), and dissolved inorganic carbon (DIC)). The full seawater CO_2 system was calculated using the carbonate speciation program CO2SYS (supporting information Table S1; see methods). To investigate the response of corals to the combined effects of coastal acidification and nutrient loading associated with SGD, skeletal cores were extracted from *Porites lobata* corals located around the discharge seep (Figure 1 and Table 1), and to the north and south of its influence, and Computerized Tomography (CT) scanned at the Woods Hole Oceanographic Institution's Computerized Tomography Scanning Facility (Crook et al., 2013). The scan images were analyzed for annual calcification and bioerosion rates using coralCT (DeCarlo & Cohen, 2016). With global warming and ocean acidification projected to compromise carbonate accretion (Fabricius et al., 2011; Gattuso et al., 2015; Hoegh-Guldberg et al., 2007), managing the compounding effects from local stressors is a top priority in reef-management. Results from this work can therefore be used to estimate changes in coral reef health under future OA and shifting off continent material flux scenarios.

Table 1
Location and Physical Characteristics of Coral Coring Locations off Kahekili Beach Park Collected in July 2013 From Porites lobata

Coral ID	Core length (cm)	Water depth (m)	Lat	Long	Lifespan	Tissue thickness (mm)	Distance offshore (m)	Distance from seep (m)	Direction from seep (°)
LobataHead01	50	<2	20°56.317′N	156°41.598′W	1970–2013	5.13	38	15	264
LobataHead02	18	<2	20°56.320′N	156°41.605′W	1992–2013	5.63	52	29	279
LobataHead03	19	<2	20°56.324′N	156°41.594′W	1987–2013	4.63	33	15	324
LobataHead04	21	<2	20°56.326′N	156°41.587′W	1983–2013	4.00	20	16	16
LobataHead05	28	<2	20°56.708′N	156°41.590′W	1984–2013	4.63	58	783	0
LobataHead06	22	<1	20°56.318′N	156°41.589′W	1978–2008[a]	n/a	23	*At seep*	*At seep*
LobataHead07	50	3	20°56.236′N	156°41.611′W	n/a	5.13	68	156	194

[a]Age of death determined by bomb-derived ^{14}C value.

2. Methods

2.1. Coral Growth Parameters

Coral cores ($n = 7$) were collected in July 2013 from the shallow reef at Kahekili in Kaanapali, west Maui, Hawaii, from scleractinian *Porites lobata* (Figure 1) in water depths of between 1 and 3 m and in the vicinity of brackish SGD "seeps" near Kahekili Beach Park (Glenn et al., 2013), approximately 0.5 km southwest of the LWRF (Table 1). All cores were collected from living *Porites* spp., except for adjacent to the seep where the coral colony was dead upon collection. Colonies were selected based on several criteria including distance from shore, distance from seep, coral shape, and water depth. Metrics of coral reef health (bioerosion, calcification, and growth rate) were quantified at the Woods Hole Oceanographic Institution's CT Scanning Facility (Crook et al., 2013) where CT scan images (supporting information Figure S1) were used to calculate the proportion of the skeleton eroded (>1 mm boring diameter) by boring organisms and calculated as the total volume of $CaCO_3$ removed relative to the total volume of the individual *Porites* coral core (Barkley et al., 2015; DeCarlo et al., 2015) using coralCT (DeCarlo & Cohen, 2016). The average growth rate reported in this study is the average linear extension rate and respective standard deviation for the length of cores analyzed per site. Pearson correlation coefficients and respective p values were calculated in Excel. Significance levels were tested at the 95% and 90% confidence level. The number of years for analysis ranged from the upper 10–26 years and was calculated as linear extension (mm) per year. The range (i.e., length of core analyzed) reflects the fact that the quality/preservation of banding was not consistent across the collection sites due to differences in boring and erosion (supporting information Figure S1). In comparison to measured bioerosion rates, predicted bioerosion rates were calculated using the equation from DeCarlo et al. (2015) where bioerosion rate $= -11.96 * \Omega_{arag} + 43.52$. Coral life spans were calculated based on annual growth rate and core length. Coral life span for the dead specimen was determined by comparing bomb-derived radiocarbon (^{14}C) values measured at five depth intervals to reference bomb-curves from Hawaii (Andrews et al., 2016). Samples were prepared for Accelerator Mass Spectrometry (AMS) radiocarbon (^{14}C) dating at the National Ocean Sciences Accelerator Mass Spectrometry (NOSAMS) facility.

2.2. Carbonate Geochemistry

Coral nitrogen isotope ($\delta^{15}N$) values were determined by collecting skeletal material (~300 mg) from the upper 4.0–5.6 mm of growth. Approximately 18 mg of material was placed into tin capsules with an approximately equivalent mass of vanadium oxide (V_2O_5) catalyst to ensure complete combustion for analysis using a Costech elemental analyzer—Isotope Ratio Mass Spectrometry (EA-IRMS) at the University of California at Santa Cruz and the USGS Stable Isotope Lab to determine $\delta^{15}N$ composition. Analytical uncertainty of 0.16‰ is reported based on replicate analysis of the international nitrogen standard, acetanilide.

2.3. Water Sample Collection and Analysis

Sampling for water at the primary seep site and in adjacent coastal waters was conducted in September 2014 and March 2016. In 2014, sampling of the submarine springs was conducted using a piezometer point directly inserted into the primary seep site (Swarzenski et al., 2012) and a 12 V peristaltic pump during both high and low tide (supporting information Table S1). At each sampling site, the salinity and temperature of the seep water and bottom water was recorded using calibrated YSI multiprobes. Seawater sampling in

March 2016 was conducted near the coral sites every 4 h over a 6 day period for nutrients and carbonate chemistry variables. A peristaltic pump was used to pump seawater from the seafloor and temperature and salinity were recorded using a calibrated YSI multimeter. In situ temperatures were also recorded from Solonist CTD Divers installed at each sampling tube (Prouty et al., 2017).

Water samples were collected for the dissolved nutrients NH_4^+, Si, PO_4^{3-}, and $[NO_3^- + NO_2^-]$ in duplicate, filtered with an in-line 0.45 μm filter (and 0.20 μm syringe filter for time series sample), and kept frozen until analysis. Nutrients were analyzed at the Woods Hole Oceanographic Institution nutrient laboratory and University of California at Santa Barbara's Marine Science Institute Analytical Laboratory via flow injection analysis for NH_4^+, Si, PO_4^{3-}, and $[NO_3^- + NO_2^-]$, with precisions of 0.6–3.0%, 0.6–0.8%, 0.9–1.3%, and 0.3–1.0% relative standard deviations, respectively. Nitrate isotope ($\delta^{15}N$ and $\delta^{18}O$) analyses were done at the University of California at Santa Cruz using the chemical reduction method (McIlvin & Altabet, 2005; Ryabenko et al., 2009) and University of California at Davis' Stable Isotope Facilities using the denitrifier method (Sigman et al., 2001). Using a Thermo Finnigan MAT 252 coupled with a GasBench II interface, isotope values are presented in per mil (‰) with respect to AIR for $\delta^{15}N$ and VSMO for $\delta^{18}O$ with a precision of 0.3–0.4‰ and 0.5–0.6‰ for $\delta^{15}N$-nitrate and $\delta^{18}O$-nitrate, respectively.

Measurement for carbonate chemistry parameters from the March 2016 collection were collected and analyzed for pH (total scale), TA, and DIC. A peristaltic pump was used to pump seawater from sampling sites through a 0.45 μm filter. Samples for pH were filtered into 30 mL optical glass cells, and were analyzed within 1 h of collection using spectrophotometric methods (Zhang & Byrne, 1996), an Ocean Optics USB2000 spectrometer and thymol blue indicator dye. Samples for TA ($\pm$1 μmol kg^{-1}) and DIC ($\pm$2 μmol kg^{-1}) were filtered into 300 mL borosilicate glass bottles, preserved by adding 100 μL saturated HgCl$_2$ solution, and bottles were pressured sealed with ground glass stoppers coated with Apiezpon grease. TA samples were analyzed using spectrophotometric methods of Yao and Byrne (1998) with an Ocean Optics USB2000 spectrometer and bromocresol purple indicator dye. DIC samples were analyzed using a UIC carbon coulometer model CM5014 and CM5130 acidification module fitted with a sulfide scrubber, and methods of Dickson et al. (2007). Dissolved oxygen ($\pm$0.1 mg L^{-1}), temperature ($\pm$ 0.01°C), and salinity ($\pm$ 0.01) were measured using a YSI multimeter calibrated daily. However, due to temperature change during water transit time within the sampling tube, in situ temperatures as recorded from Solonist CTD Divers were reported and used to temperature correct pH and perform CO2SYS calculations.

Certified reference materials (CRM) for TA and DIC analyses were from the Marine Physical Laboratory of Scripps Institution of Oceanography (A. Dickson, personal communication, 2016). Duplicate or triplicate analyses were performed on at least 10% of samples, yielding a mean precision of ~1 and ~2 μmol kg^{-1} for TA and DIC analyses, respectively. For low salinity (<10) water samples collected directly from the seep, discrete DIC samples were measured on an Apollo SciTech AS-C3 DIC autoanalyzer via sample acidification followed by nondispersive infrared CO$_2$ detection using a LiCOR 7000. The instrument was calibrated with certified reference material (CRM) from Dr. A.G. Dickson at the Scripps Institution of Oceanography. A modified Gran titration procedure by Wang and Cai (2004) was used to determine TA with an Apollo SciTech AS-ALK2 automated titrator and CRM-calibrated HCl at 25.0°C. The full seawater CO$_2$ system was calculated with measured salinity, temperature, nutrients (phosphate and silicate), TA, and pH data using an Excel Workbook Macro translation of the original CO2SYS program (Pierrot et al., 2006). The CO2SYS 2.0 program was run with dissociation constants K$_1$ and K$_2$ from Mehrbach et al. (1973) refit by Dickson and Millero (1987) and KSO4 from Dickson (1990). The aragonite saturation state (Ω_{arag}) was defined as the ratio of [CO$_3^{2-}$] and [Ca^{2+}] divided by the aragonite solubility product (K$_{sp}$). The concentration of calcium [Ca^{2+}] was assumed to be proportional to the salinity, and the carbonate concentration was calculated from DIC, pH, and the values of K$_1$ and K$_2$ (Pierrot et al., 2006).

3. Results

3.1. Seawater Carbonate Chemistry

The 6 day continuous sampling in March 2016 revealed dynamic changes in the chemistry of seawater adjacent to the primary seep site, and captured the level of exposure of corals to variable pH and nutrient conditions (Figure 2 and supporting information Table S1). From 16 to 19 March 2016, salinity increased and nutrient concentrations steadily declined, while pH values increased. From 21 to 24 March 2016, salinity
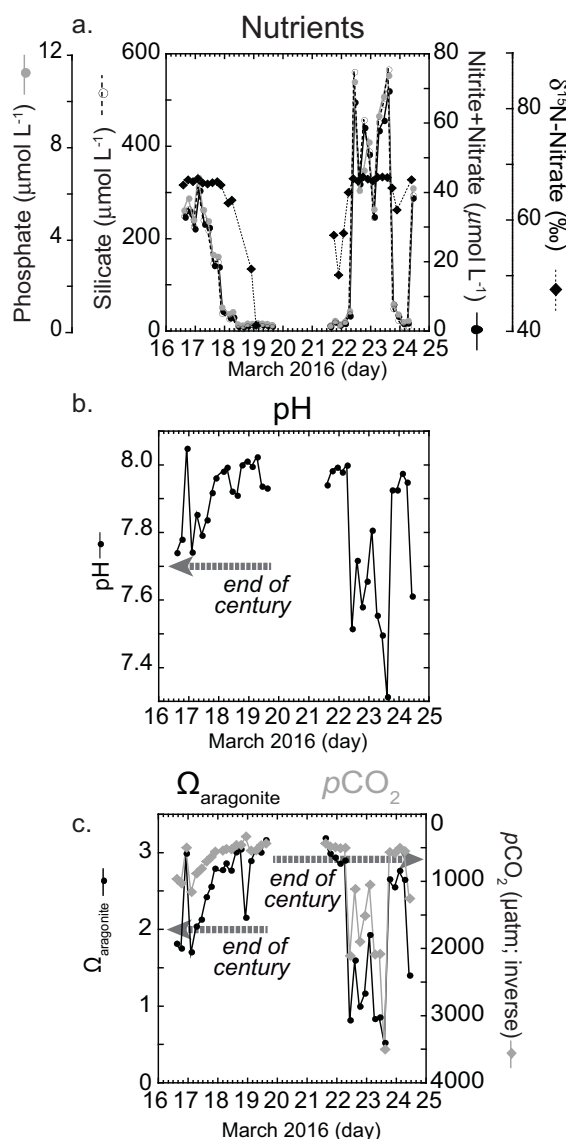
Figure 2. Results of time series of seawater chemistry variables over a 6 day period collected from bottom water near the seep site on the nearshore reef (20°56.31660′, −156°41.59080′) every 4 h. (a) Dissolved nutrient (nitrate + nitrite, phosphate, and silicate) concentrations (μmol L^{-1}), and nitrate stable nitrogen isotopes (δ^{15}N-nitrate; ‰); (b) temperature corrected pH (total scale); and (c) calculated carbonate parameters for aragonite saturation state (Ω_{arag}) and pCO$_2$ (μatm; inverted) based on TA-pH pairwise and measured salinity, temperature, nutrients (phosphate and silicate) data. End-of-century projections according to the "business as usual" RCP8.5 scenario for pH (reduction by 0.4 units), Ω_{arag} (2.0), and pCO$_2$ (750 μatm) (Fabricius et al., 2011).

decreased and nutrient concentrations increased by five orders of magnitude as pH fell, reaching values as low as 7.36 at the primary seep site (Figures 2a and 2b). During this time, DIC and TA values increased, and Ω_{arag} fell below saturation for approximately 15% of the time at the primary seep site (Figure 2c and supporting information Table S1). All carbonate parameters adjacent to the primary seep site behaved conservatively with respect to salinity (supporting information Figure S2), demonstrating the tight coupling between nutrients and pH and freshened seep water input, consistent with earlier work documenting lower pH, nutrient enriched SGD derived seep water (Glenn et al., 2013; Swarzenski et al., 2012, 2016). Nutrients, TA, and DIC continued to covary with salinity at values greater than 33, suggesting that these stressors may have greater potential to impact those corals away from the seep. Although the salinity was extremely low at the seep, by the time affected waters reached corals only meters away, it had become well mixed with respect to salinity, and most corals in the vicinity of the seep were experiencing salinities ranging from 34 to 36 (supporting information Table S1). However, nutrients can impact the corals "downstream" because they are assimilated rapidly, fueling productivity that was likely driving the bioerosion (e.g., Carreiro-Silva et al., 2005, 2009). These conditions clearly demonstrate that SGD is the primary source of elevated bottom water nutrient concentrations and dramatically under-saturated seawater ($\Omega_{arag} < 1$), corresponding to seawater pCO$_2$ values greater than 1500 μatm (Figure 2).

3.2. Coral Cores

Measured bioerosion rates and percent volume erosion were highest at the coral site adjacent to the active SGD seep, and lowest at the coral site furthest from the seep, with bioerosion rates ranging between 23 and 99 mg cm^{-2} yr^{-1} (Table 2). However, the bioerosion rate of LobataHead06 may be an overestimate given that the core was collected from a dead specimen. The correlation between coral bioerosion rates and percent volume erosion relative to distance to the seep ($r = -0.69$ and -0.62, respectively) was significant at the 90% confidence level (Table 3). In addition, correlations between bioerosion rate and percent bioerosion volume and seawater parameters (Ω_{arag}, pH, and nitrate) were statistically significant ($p < 0.05$). Growth rates ranged from 0.69 ± 0.10 to 1.17 ± 0.26 cm yr^{-1}, and calcification rates ranged from 0.67 to 1.10 g cm^{-2} yr^{-1} (Table 2). Calcification rates were correlated to distance from shore ($r = 0.72$; $p \leq 0.05$; Table 3). Neither growth parameter, however, was statistically correlated to bioerosion rates however seawater parameters were correlated to growth rate at the 90% confidence level.

To investigate whether the corals assimilate SGD nitrate, the δ^{15}N composition of the coral tissue from the upper 4.0–5.6 mm of coral growth was analyzed. Coral δ^{15}N values were highest closest to the seep site (17.08 ± 0.40‰; Table 2), and decreased with distance away from the seep ($r = -0.58$; $p = 0.09$) and from shore ($r = -0.88$; $p < 0.05$; Table 3). With the exception of one coral head, all tissue δ^{15}N collected from corals near the primary seep zone, referred to as the "dead zone," were enriched relative to the north and south coral sites according to a one-way analysis of variance (ANOVA; $F_{(6,50)} = 136.1$; $p < 0.0001$; supporting information Figure S3). Coral δ^{15}N values were also positively correlated to percent volume bioerosion ($r = 0.68$, $p = 0.07$; supporting information Figure S3), and inversely correlated with calcification rates ($r = -0.70$, $p = 0.06$; Table 3).

4. Discussion

At the Kahekili site off the west coast of Maui, sustained SGD is rich in nutrients and also has lower pH (average 7.5 ± 1.7). As a result of this SGD, the surrounding corals are exposed to multiple associated stressors,

Table 2

Coral Growth Parameters Quantified by Computerized Tomography (CT) for Growth Rate ($\pm$SD; cm yr^{-1}), Density (g cm^{-3}), and Calcification Rates (g cm^{-2} yr^{-1}), Percent Volume Erosion (%), Measured Bioerosion Rate (mg cm^{-2} yr^{-1}), Predicted Bioerosion Rate (mg cm^{-2} yr^{-1}) Based on DeCarlo et al. (2015); Bioerosion Rate = $-11.96*\Omega_{arag} + 43.52$), and Average ($\pm$STD) Coral Tissue Nitrogen Isotope (δ^{15}N; ‰) Values

Coral head	Growth rate	Density	Calcification	Volume bioerosion	Bioerosion rate	Predicted bioerosion rate	δ^{15}N	Ω_{arag}	pH	Salinity	Nitrate
LobataHead01 (n = 24 years)	1.17 ± 0.26	1.04	1.10	6.57	72.32	n/a	11.29 ± 1.76 (n = 9)	n/a	n/a	n/a	n/a
LobataHead02 (n = 21 years)	0.88 ± 0.06	1.08	0.94	5.94	56.03	7.04	8.44 ± 0.12 (n = 12)	3.05 ± 0.10	8.00 ± 0.02	35.19 ± 0.87	0.16 ± 0.10
LobataHead03 (n = 26 years)	0.72 ± 0.10	0.99	0.71	12.48	89.07	n/a	10.87 ± 0.45 (n = 9)	n/a	n/a	n/a	n/a
LobataHead04 (n = 20 years)	0.72 ± 0.16	1.01	0.67	5.92	39.87	7.04	14.62 ± 0.23 (n = 9)	3.05 ± 0.17	8.01 ± 0.03	34.98 ± 0.99	0.41 ± 0.18
LobataHead05 (n = 13 years)	0.95 ± 0.11	1.15	1.02	2.20	22.58	6.92	7.50 ± 0.19 (n = 9)	3.06 ± 0.11	8.01 ± 0.02	35.36 ± 1.10	0.19 ± 0.11
LobataHead06 (n = 10 years)	0.69 ± 0.10	1.07	0.68	14.63	99.15	16.37	17.08 ± 0.40 (n = 3)	2.27 ± 0.81	7.85 ± 0.17	28.57 ± 7.79	20.35 ± 23.32
LobataHead07	n/a	n/a	n/a	n/a	n/a	n/a	8.17 ± 0.19 (n = 6)	n/a	n/a	n/a	n/a

Note. LobataHead07 was not analyzed for growth parameters prior to subsectioning for geochemical analysis. Seawater chemistry parameters (Ω_{arag}, temperature corrected-pH, salinity, and nitrate (μmol L^{-1}) are reported as average ($\pm$SD; $n = 37$) based on 6 day sampling period in March 2016.

including nitrate concentrations up to 50 times higher than ambient seawater, and lower pH bottom water. Additional stressors from SGD, including reduced salinity at the primary seep site, and elevated TA and DIC concentrations can impact the corals by changes in photosynthesis, respiration, as well as increased bleaching and mortality (e.g., Ferrier-Pages et al., 1999). We did not observe, however, the salinity extremes away from the seep that would have caused physiological stress/tissue loss/damage, yet increased rates of bioerosion were observed. An increase in TA and DIC can drive a shift from positive net community calcification to net negative community calcification, or net dissolution relative to calcification (Deffeyes, 1965). With expected reductions in calcification rates predicted under higher pCO$_2$ conditions (Bernstein et al., 2016; Shamberger et al., 2011; Shaw et al., 2012), the interplay of bioeroding organisms under reduced community calcification could enhance both chemical and mechanical bioerosion rates.

Bioerosion rates from dead pieces of the massive coral *Porites* spp. skeleton from along a natural pH gradient in Kāne'ohe Bay, Oahu, reported rates from 2 to 91 mg cm^{-2} yr^{-1} (Silbiger et al., 2016), with the upper range in rates comparable to those observed closet to the SGD seep at Kahekili. Comparing bioerosion rates remains

Table 3

Pearson-Product Correlation Coefficients (r; Bold $p \le 0.05$; Italics $p \le 0.10$) between Average Coral Reef Growth Parameters (Growth Rate, Density, %Volume Bioerosion, Calcification, and Lifespan), Location (Distance From Shore and Primary Seep Site), Average Coral δ^{15}N-Nutrient Loading Proxy, and Average Seawater Variables (Ω_{arag}, pH, and Nitrate)

	Coral tissue δ^{15}N	Growth rate	Density	% Volume bioerosion	Calcification	Bioerosion rate	Lifespan	Distance from shore	Distance from seep	Ω_{arag}	pH
Average growth rate	−0.53										
Overall density	−0.45	0.33									
Bioerosion % volume	*0.68*	−0.57	−0.51								
Average calcification	−0.70	**0.95**	0.54	−0.66							
Bioerosion rate	0.55	−0.27	−0.51	**0.94**	−0.39						
Lifespan	0.29	*0.60*	−0.09	0.02	0.38	0.20					
Distance from shore	**−0.88**	0.49	**0.81**	−0.68	**0.72**	*−0.61*	−0.22				
Distance from seep	*−0.58*	0.26	**0.80**	−0.62	0.44	*−0.69*	−0.08	**0.83**			
Ω_{arag}	**−0.66**	*0.64*	0.05	**−0.95**	0.57	**−0.91**	−0.55	0.53	0.37		
pH	**−0.72**	*0.62*	0.05	**−0.95**	0.54	**−0.93**	−0.50	0.50	0.39	**0.99**	
Nitrate	**0.74**	−0.64	−0.05	**0.94**	−0.57	**0.91**	0.56	−0.53	0.36	**0.99**	**0.99**

difficult, however, due to heterogeneity in bioeroding communities (e.g., chemical versus mechanical, internal versus external, microbioeroders versus macrobioeroders), as well as differences in environmental factors (e.g., hydrodynamics, temperature, etc.) and analytical approaches (e.g., SEM, grazing scars). For example, comparing bioerosion rates from carbonate blocks may not be an appropriate comparison given different bioeroding communities of dead versus alive substrate (e.g., Hutchings, 1986; Sammarco et al., 1987). In order to reduce uncertainty that could be an artifact from different field and/or analytical approach, rates derived by the same techniques as reported here were compared. Bioerosion rates from 15 sites across the tropical Pacific range from 0 to 68 mg cm^{-2} yr^{-1} (supporting information Table S2), with bioerosion rates at Kahekili up to 30 mg cm^{-2} yr^{-1} higher than measured elsewhere in the basin. Elevated bioerosion rates at Kahekili are consistent with findings from Silbiger et al. (2017) that reported the highest average bioerosion rate and lowest net accretion rate across the Hawaiian Archipelago at the Kahekili study site. In comparison to measured bioerosion rates, we calculated predicted bioerosion rates using the equation from DeCarlo et al. (2015) where bioerosion rate = −11.96 * Ω_{arag} + 43.52. Based on this computation, greater-than-predicted bioerosion rates for an oligotrophic setting in the Pacific were measured at Kahekili (Figure 3). In other words, measured coral bioerosion rates at Kahekili are up to 8 times greater than expected for corals growing away from land-based sources of pollution (DeCarlo et al., 2015; Table 2).

Although our study did not quantify bioerosion rates by microborers per se, chemical bioerosion by microborers will contribute to net bioerosion rates by weakening of coral skeleton (Tribollet et al., 2009) as well as by grazing from fish and echinoids (Perry et al., 2014). Given the elevated nutrient concentrations at Kahekili, the data appear to indicate that eutrophication is driving elevated bioerosion rates at Kahekili. This finding is consistent with previous work showing increased bioeroding communities with increased nutrient concentrations and declining water quality (e.g., Carreiro-Silva et al., 2005, 2009; Edinger et al., 2000; Holmes et al., 2000). At Kahekili, large-scale ephemeral blooms of green alga (Smith et al., 2005) can act to stimulate bioeroders, with both filter feeders and photoautotrophs capitalizing on nutrients in both the dissolved and particulate form. Microbioeroders can therefore interact with different bioeroding communities and
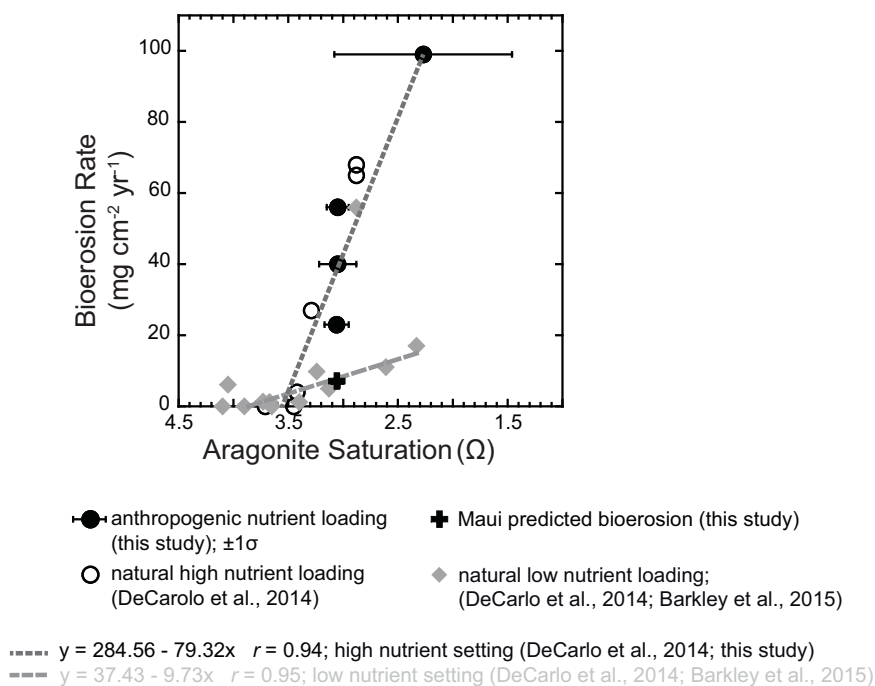

Figure 3. Relationship between aragonite saturation state ($\Omega_{arag} \pm 1\sigma$; inverted axis) measured in March 2016 and coral bioerosion (mg cm^{-2} yr^{-1}) from west Maui exposed to anthropogenic nutrient loading (black circles), naturally high-nutrient (open circles) and low-nutrient (gray diamonds) reefs across the Pacific Basin (Barkley et al., 2015; DeCarlo et al., 2015). The predicted bioerosion rate for Maui (black cross) was calculated using the equation bioerosion rate = −11.96* Ω_{arag} + 43.52 (DeCarlo et al., 2015) and a calculated Ω value of 3.06 based on offshore sampling site (∼70 m), south of the seep (∼150 m) site with nitrate concentrations <0.20 μmol L^{-1}.

contribute to the bioerosion loop (Schönberg et al., 2017). It is also important to point out the succession dynamics of bioeroders on marine carbonate budgets, whereby one taxon group prepares the substrate for the next bioeroder community (e.g., Hutchings, 1986, 2011; Kiene & Hutchings, 1994; Scott & Risk, 1988), including providing crevices for the intrusion of bivalves (e.g., Morton, 1983; Morton & Scott, 1980). In addition, endolithic algae play an important role in erosive and early digenetic process (e.g., Kobluk & James, 1979; Kobluk & Risk, 1977). Vulnerability to physical erosion is further enhanced by bioerosion whereby the coral colony's ability to withstand wave shock and storm waves is reduced (e.g., Hein & Risk, 1975; Highsmith et al., 1980; Scott & Risk, 1988; Tunnicliffe, 1979, 1981). The degree of degradation and coral mortality has been linked to turf algal competition, with the "dead zone" characterized by clustered patches of variable degrees of degradation along the length of the reef at Kahekili Beach Park (Ross et al., 2012). Increased mortality will therefore further facilitate bioerosion by increasing exposed carbonate structure on the corals. The decrease in abundance of reef grazing herbivores at Kahekili (Williams et al., 2016) may also be a contributing factor to the establishment of certain bioeroders (Paddack et al., 2006).

Elevated coral δ^{15}N values indicate not only eutrophication, but also a sewage nitrogen source enriched in ^{15}N (Heaton, 1986). Input of such an effluent to Maui's coral reef ecosystem has been documented by elevated algae δ^{15}N values, with the highest algae δ^{15}N values found in close proximity to the LWRF, yielding values of up to 43.3 $\pm$ 0.08‰, indicative of wastewater effluent (Dailer et al., 2010). Those results are consistent with seawater δ^{15}N-nitrate values measured near the seep that were typically greater than 65‰ (Figure 2a). The elevated coral and nitrate δ^{15}N ratios are therefore a function of both denitrification processes within the SGD pathway and an elevated δ^{15}N signature of the effluent source (Fackrell et al., 2016; Kendall, 1998). The LWRF processes approximately 12.8 million L d^{-1} of wastewater effluent with estimated nitrogen loading of 79–97 kg d^{-1} (Glenn et al., 2013). Based on SGD rates derived for the primary seep site (Swarzenski et al., 2016) and nitrate concentrations measured directly from the discharging seep water (supporting information Table S1), the freshened seep water is estimated to deliver approximately 714 mol d^{-1} nitrate. Although seawater above the seep is an admixture of SGD and ambient seawater, exposure of nutrient-laden/low pH freshwater occurred approximately 8 h d^{-1}, during the semidiurnal low tides when salinity values typically dropped below 10 and maximum SGD rates were observed (Glenn et al., 2013). To exacerbate the exposure to contaminated nutrient-enriched effluent, the direction of maximum flow during the transition from high to low tide were dominantly offshore (Swarzenski et al., 2016), transporting nutrient-rich water from the nearshore seeps towards the reef.

The elevated coral δ^{15}N values not only indicate that coral δ^{15}N appears to be a reliable tracer of nutrient loading and nitrate assimilation, but also further demonstrates a link between exposure to elevated nutrient levels and coral health given the observed increased bioerosion rates and decreased calcification rates at sites closest to the primary seep. In comparison, coral bioerosion rates and δ^{15}N values were lower at sites away from the primary seep, consistent with a decrease in nitrate flux (245 mol d^{-1}) 85 m offshore from the primary seep site where measured SGD rates decreased to 30 cm d^{-1} (Swarzenski et al., 2016). Enhanced nutrient loading from greater SGD nitrate fluxes can therefore increase abundance of bioeroding communities (Carreiro-Silva et al., 2005, 2009; Edinger et al., 2000; Holmes et al., 2000). Teasing apart the different stressors from SGD is difficult given that pH, nutrients, TA, and DIC covary with salinity. Any stressor that reduces live tissue coverage can ultimately increase bioerosion rates due to increased area of exposed substrate. At a salinity greater than 33, however, the relation between pH and salinity seems to break down, whereas TA, DIC, and nutrients continue to covary with salinity (supporting information Figure S2), indicating that these stressors may have greater potential to impact corals growing away from the seep. Mesocosm experiments that can manipulate these individual stressors in a controlled environment (Wiedenmann et al., 2013) therefore represent important complimentary studies to the field-based results presented here.

5. Conclusion

Based on observations from this site off west Maui, land-based sources of pollution, in synergy with changing ocean conditions on a global scale, interact to deleteriously influence coral reef health in the nearshore environment. Our results confirm how valuable nearshore coral reef ecosystems—the cornerstone of Hawaiian tourism, shoreline protection, and local fisheries—are affected by land-based sources of pollution that

are also magnified by effects of coastal acidification. The range of exposure of reefs living in the vicinity of the SGD seep at Kahekili are comparable to end of century pCO_2 projections (Fabricius et al., 2011; Figure 2c). With the largest decrease in Ω projected for the tropics (Gattuso et al., 2015), coral reefs are extremely vulnerable to CO_2-related threats given the synergistic drivers responsible for present day coral degradation. Bioerosion rates at our study site, however, are much greater than predicted for an oligotrophic setting, suggesting that eutrophication exacerbates ocean acidification and bioerosion of corals, causing coral reef collapse much sooner in the future than currently predicted (van Hooidonk et al., 2014). With many of Maui's coral reefs in significant decline (Rodgers et al., 2015; Yates et al., 2017) and recent coral bleaching events leading to increased coral mortality (Sparks et al., 2016), reducing any stressors at a local scale—especially ones that can be readily attenuated with proactive resource management of nutrients—is imperative to sustaining future coral reef ecosystems and planning for resiliency.

References

Amato, D. W., Bishop, J. M., Glenn, C. R., Dulai, H., & Smith, C. M. (2016). Impact of submarine groundwater discharge on marine water quality and reef biota of Maui. *PLoS ONE*, *11* (11), e0165825. https://doi.org/doi:10.1371/journal.pone.0165825

Anderson, D. M., Glibert, P. M., & Burkholder, J. M. (2002). Harmful algal blooms and eutrophication: Nutrient sources, composition and consequences. *Estuaries*, *25*, 562–584. https://doi.org/10.1007/BF02804901

Andrefouet, S., Mumby, P. J., McField, M., Hu, C., & Muller-Karger, F. E. (2002). Revisiting coral reef connectivity. *Coral Reefs*, *21*(1), 43–48. https://doi.org/10.1007/s00338-001-0199-0

Andrews, A. H., Siciliano, D., Potts, D. C., DeMartini, E. E., & Covarrubias, S. (2016). Bomb radiocarbon and the Hawaiian Archipelago: Coral, otoliths, and seawater. *Radiocarbon*, *58*(3), 531–548. https://doi.org/10.1017/RDC.2016.32

Anthony, K. R. N., Kline, D. I., Diaz-Pulido, G., Dove, S., & Hoegh-Guldberg, O. (2008). Ocean acidification causes bleaching and productivity loss in coral reef builders. *Proceedings of the National Academy of Sciences United States of America*, *105*(45), 17442–17446. https://doi.org/10.1073/pnas.0804478105

Ban, S. S., Graham, N. A. J., & Connolly, S. R. (2014). Evidence for multiple stressor interactions and effects on coral reefs. *Global Change Biology*, *20*(3), 681–697. https://doi.org/10.1111/gcb.12453

Barkley, H. C., Cohen, A. L., Golbuu, Y., Starczak, V. R., DeCarlo, T. M., & Shamberger, K. E. F. (2015). Changes in coral reef communities across a natural gradient in seawater pH. *Science Advances*, *1*(5), e1500328. https://doi.org/10.1126/sciadv.1500328

Bernstein, W. N., Hughen, K. A., Langdon, C., McCorkle, D. C., & Lentz, S. J. (2016). Environmental controls on daytime net community calcification on a Red Sea reef flat. *Coral Reefs*, *35*(2), 697–711.

Bienfang, P. (1980). Water quality characteristics of Honokohau Harbor: A subtropical embayment affected by groundwater intrusion. *Pacific Science*, *34*(3), 279–291.

Bishop, J. M., Glenn, C. R., Amato, D. W., & Dulai, H. (2015). Effect of land use and groundwater flow path on submarine groundwater discharge nutrient flux. *Journal of Hydrology: Regional Studies*, *11*, 194–218. https://doi.org/10.1016/j.ejrh.2015.10.008

Bruno, J. F., Petes, L. E., Harvell, C. D., & Hettinger, A. (2003). Nutrient enrichment can increase the severity of coral diseases. *Ecology Letters*, *6*, 1056–1061. https://doi.org/10.1046/j.1461-0248.2003.00544.x

Carreiro-Silva, M., McClanahan, T. R., & Kiene, W. E. (2005). The role of inorganic nutrients and herbivory in controlling microbioerosion of carbonate substratum. *Coral Reefs*, *24*(2), 214–221. https://doi.org/10.1007/s00338-004-0445-3

Carreiro-Silva, M., McClanahan, T. R., & Kiene, W. E. (2009). Effects of inorganic nutrients and organic matter on microbial euendolithic community composition and microbioerosion rates. *Marine Ecology Progress Series*, *392*, 1–15.

Cochran, S. A., Gibbs, A. E., & White, D. J. (2014). Benthic habitat map of the U.S. Coral Reef Task Force Watershed Partnership Initiative Kā'anapali priority study area and the State of Hawai'i Kahekili Herbivore Fisheries Management Area, west-central Maui, Hawai'i. (U.S. Geol. Surv. Open-File Rep. 2014-1129, 42 p.). Reston, VA: U.S. Geological Survey.

Crook, E. D., Cohen, A. L., Rebolledo-Vieyra, M., Hernandez, L., & Paytan, A. (2013). Reduced calcification and lack of acclimatization by coral colonies growing in areas of persistent natural acidification. *Proceedings of the National Academy of Sciences United States of America*, *110*(27), 11044–11049. https://doi.org/10.1073/pnas.1301589110

Crook, E. D., Potts, D., Rebolledo-Vieyra, M., Hernandez, L., & Paytan, A. (2012). Calcifying coral abundance near low-pH springs: Implications for future ocean acidification. *Coral Reefs*, *31*(1), 239–245. https://doi.org/10.1007/s00338-011-0839-y

Dailer, M. L., Knox, R. S., Smith, J. E., Napier, M., & Smith, C. M. (2010). Using δ^{15}N values in algal tissue to map locations and potential sources of anthropogenic nutrient inputs on the island of Maui, Hawai'i, USA. *Marine Pollution Bulletin*, *60*(5), 655–671. https://doi.org/10.1016/j.marpolbul.2009.12.021

Dailer, M. L., Ramey, H. L., Saephan, S., & Smith, C. M. (2012). Algal δ^{15}N values detect a wastewater effluent plume in nearshore and offshore surface waters and three-dimensionally model the plume across a coral reef on Maui, Hawai'i, USA. *Marine Pollution Bulletin*, *64*(2), 207–213. https://doi.org/10.1016/j.marpolbul.2011.12.004

DeCarlo, T. M., & Cohen, A. L. (2016). coralCT: Software tool to analyze computerized tomography (CT) scans of coral skeletal cores for calcification and bioerosion rates. *Zenodo*. https://doi.org/10.5281/zenodo.57855

DeCarlo, T. M., Cohen, A. L., Barkley, H. C., Cobban, Q., Young, C., Shamberger, K. E., . . . Golbuu, Y. (2015). Coral macrobioerosion is accelerated by ocean acidification and nutrients. *Geology*, *43*(1), 7–10. https://doi.org/10.1130/G36147.1

Deffeyes, K. S. (1965). Carbonate equilibria: A graphic and algebraic approach. *Limnology and Oceanography*, *10*(3), 412–426. https://doi.org/10.4319/lo.1965.10.3.0412

Dickson, A. G. (1990). Thermodynamics of the dissociation of boric acid in synthetic seawater from 273.15 to 318.15 K. *Deep Sea Research Part A: Oceanographic Research Papers*, *37*(5), 755–766. https://doi.org/10.1016/0198-0149(90)90004-F

Dickson, A. G., & Millero, F. J. (1987). A comparison of the equilibrium constants for the dissociation of carbonic acid in seawater media. *Deep Sea Research Part A: Oceanographic Research Papers*, *34*(10), 1733–1743. https://doi.org/10.1016/0198-0149(87)90021-5

Dickson, A. G., Sabine, C. L., & Christian, J. R. (2007). *Guide to best practices for ocean CO2 measurements*. (Vol. 3, 191 pp.). Sidney, BC: PICES Special Publication.

Dimova, N. T., Swarzenski, P. W., Dulaiova, H., & Glenn, C. R. (2012). Utilizing multichannel electrical resistivity methods to examine the dynamics of the fresh water–seawater interface in two Hawaiian groundwater systems. *Journal of Geophysical Research*, *117*, C02012. https://doi.org/10.1029/2011JC007509

Edinger, E. N., Limmon, G. V., Jompa, J., Widjatmoko, W., Heikoop, J. M., & Risk, M. J. (2000). Normal coral growth rates on dying reefs: Are coral growth rates good indicators of reef health? *Marine Pollution Bulletin*, *40*(5), 404–425.

Enochs, I. C., Manzello, D. P., Kolodziej, G., Noonan, S. H. C., Valentino, L., & Fabricius, K. E. (2016). Enhanced macroboring and depressed calcification drive net dissolution at high-CO_2 coral reefs. *Proceedings of the Royal Society B: Biological Sciences*, *283*(1842), https://doi.org/10.1098/rspb.2016.1742

Fabricius, K. E. (2005). Effects of terrestrial runoff on the ecology of corals and coral reefs: Review and synthesis. *Marine Pollution Bulletin*, *50*, 125–146. https://doi.org/10.1016/j.marpolbul.2004.11.028

Fabricius, K. E., Langdon, C., Uthicke, S., Humphrey, C., Noonan, S., De'ath, G., . . . Lough, J. M. (2011). Losers and winners in coral reefs acclimatized to elevated carbon dioxide concentrations. *Nature Climate Change*, *1*(3), 165–169. https://doi.org/10.1038/nclimate1122

Fackrell, J. K., Glenn, C. R., Popp, B. N., Whittier, R. B., & Dulai, H. (2016). Wastewater injection, aquifer biogeochemical reactions, and resultant groundwater N fluxes to coastal waters: Kā'anapali, Maui, Hawai'i. *Marine Pollution Bulletin*, *110*(1), 281–292. https://doi.org/10.1016/j.marpolbul.2016.06.050

Ferrario, F., Beck, M. W., Storlazzi, C. D., Micheli, F., Shepard, C. C., & Airoldi, L. (2014). The effectiveness of coral reefs for coastal hazard risk reduction and adaptation. *Nature Communications*, *5*, 3794. https://doi.org/10.1038/ncomms4794

Ferrier-Pages, C., Gattuso, J. P., & Jaubert, J. (1999). Effect of small variations in salinity on the rates of photosynthesis and respiration of the zooxanthellate coral *Stylophora pistillata*. *Marine Ecology Progress Series*, *181*, 309–314.

Gattuso, J. P., Magnan, A., Billé, R., Cheung, W. W. L., Howes, E. L., Joos, F., . . . Turley, C. (2015). Contrasting futures for ocean and society from different anthropogenic CO_2 emissions scenarios. *Science*, *349*(6243), aac4722. https://doi.org/10.1126/science

Glenn, C. R., Whittier, R. B., Dailer, M. L., Dulaiova, H., El-Kadi, A. I., Fackrell, J., . . . Sevadjian, L. (2013). Lahaina Groundwater Tracer Study—Lahaina, Maui, Hawaii (final report, 502 p.). Honolulu, HI: State of Hawaii Department of Health, the U.S. Environmental Protection Agency, and the U.S. Army Engineer Research and Development Center.

Glynn, P. W., & Manzello, D. P. (2015). Bioerosion and coral reef growth: A dynamic balance. In C. Birkeland (Ed.), *Coral reefs in the Anthropocene* (pp. 67–97). Dordrecht, the Netherlands: Springer.

Heaton, T. H. E. (1986). Isotopic studies of nitrogen pollution in the hydrosphere and atmosphere: A review. *Chemical Geology: Isotope Geoscience Section*, *59*, 87–102.

Hein, F. J., & Risk, M. J. (1975). Bioerosion of coral heads: Inner patch reefs, Florida reef tract. *Bulletin of Marine Science*, *25*(1), 133–138.

Highsmith, R. C., Riggs, A. C., & D'antonio, C. M. (1980). Survival of hurricane-generated coral fragments and a disturbance model of reef calcification/growth rates. *Oecologia*, *46*(3), 322–329.

Hoegh-Guldberg, O., Mumby, P. J., Hooten, A. J., Steneck, R. S., Greenfield, P., Gomez, E., . . . Hatziolos, M. E. (2007). Coral reefs under rapid climate change and ocean acidification. *Science*, *318*, 1737–1742. https://doi.org/10.1126/science.1152509

Holmes, K. E., Edinger, E. N., Limmon, G. V., & Risk, M. J. (2000). Bioerosion of live massive corals and branching coral rubble on Indonesian coral reefs. *Marine Pollution Bulletin*, *40*(7), 606–617.

Howarth, R., Anderson, D., Cloern, J., Elfring, C., Hopkinson, C., Lapointe, B., . . . Walker, D. (2000). Nutrient pollution of coastal rivers, bays, and seas. *Issues in Ecology*, *7*, 1– 15.

Hughes, T. P., Baird, A. H., Bellwood, D. R., Card, M., Connolly, S. R., Folke, C., . . . Roughgarden, J. (2003). Climate change, human impacts, and the resilience of coral reefs. *Science*, *301*(5635), 929–933. https://doi.org/10.1126/science.1085046

Hughes, T. P., Rodrigues, M. J., Bellwood, D. R., Ceccarelli, D., Hoegh-Guldberg, O., McCook, L., . . . Willis, B. (2007). Phase shifts, serbivory, and the resilience of coral reefs to climate change. *Current Biology*, *17*(4), 360–365. https://doi.org/10.1016/j.cub.2006.12.049

Hunt, C. D., Jr., & Rosa, S. N. (2009). A multitracer approach to detecting wastewater plumes from municipal injection wells in nearshore marine waters at Kihei and Lahaina, Maui, Hawaii (U.S. Geol. Surv. Sci. Invest. Rep. 2009–5253, 166 p.). Reston, VA: U.S. Geological Survey.

Hutchings, P. A. (1986). Biological destruction of coral reefs. *Coral Reefs*, *4*(4), 239–252. https://doi.org/10.1007/BF00298083

Hutchings, P. (2011). Bioerosion. In D. Hopley (Eds.), *Encyclopedia of modern coral reefs* (pp. 139–156). Berlin, Germany: Springer.

Kendall, C. (1998). Tracing nitrogen sources and cycling in catchments. In C. Kendall & J. J. McDonnell (Eds.), *Isotope tracers in catchment hydrology* (pp. 519–576). Amsterdam: Elsevier.

Kiene, W. E., & Hutchings, P. A. (1994). Bioerosion experiments at Lizard Island, Great Barrier Reef. *Coral Reefs*, *13*(2), 91–98.

Kleypas, J. A., Buddemeier, R. W., Archer, D., Gattuso, J.-P., Langdon, C., & Opdyke, B. N. (1999). Geochemical consequences of increased atmospheric carbon dioxide on coral reefs. *Science*, *284*(5411), 118–120. https://doi.org/10.1126/science.284.5411.118

Knowlton, N., & Jackson, J. B. C. (2008). Shifting baselines, local impacts, and global change on coral reefs. *PLoS Biology*, *6*(2), e54. https://doi.org/10.1371/journal.pbio.0060054

Kobluk, D. R., & James, N. P. (1979). Cavity-dwelling organisms in Lower Cambrian patch reefs from southern Labrador. *Lethaia*, *12*(3), 193–218.

Kobluk, D. R., & Risk, M. J. (1977). Calcification of exposed filaments of endolithic algae, micrite envelope formation and sediment production. *Journal of Sedimentary Research*, *47*(2), 517–528.

Lapointe, B. E., Barile, P. J., Littler, M. M., & Littler, D. S. (2005). Macroalgal blooms on southeast Florida coral reefs. II. Cross-shelf d[15]N values provide evidence of widespread sewage enrichment. *Harmful Algae*, *4*, 1106–1122. https://doi.org/10.1016/j.hal.2005.06.004

McIlvin, M. R., & Altabet, M. A. (2005). Chemical conversion of nitrate and nitrite to nitrous oxide for nitrogen and oxygen isotopic analysis in freshwater and seawater. *Analytical Chemistry*, *77*(17), 5589–5595. https://doi.org/10.1021/ac050528s

Mehrbach, C., Culberson, C. H., Hawley, J. E., & Pytkowicx, R. M. (1973). Measurement of the apparent dissociation constants of carbonic acid in seawater at atmospheric pressure. *Limnology and Oceanography*, *18*(6), 897–907. https://doi.org/10.4319/lo.1973.18.6.0897

Morton, B., & Scott, P. J. B. (1980). Morphological and functional specializations of the shell, musculature and pallial glands in the Lithophaginae (Mollusca: Bivalvia). *Journal of Zoology*, *192*, 179–203.

Nelson, C. E., Donahue, M. J., Dulaiova, H., Goldberg, S. J., La Valle, F. F., Lubarsky, K., . . . Thomas, F. I. M. (2015). Fluorescent dissolved organic matter as a multivariate biogeochemical tracer of submarine groundwater discharge in coral reef ecosystems. *Marine Chemistry*, *177*(Part 2), 232–243.

Osorno, A., Peyrot-Clausade, M., & Hutchings, P. A. (2005). Patterns and rates of erosion in dead Porites across the Great Barrier Reef (Australia) after 2 years and 4 years of exposure. *Coral Reefs*, *24*(2), 292–303.

Paddack, M. J., Cowen, R. K., & Sponaugle, S. (2006). Grazing pressure of herbivorous coral reef fishes on low coral-cover reefs. *Coral Reefs*, *25*(3), 461–472. https://doi.org/10.1007/s00338-006-0112-y

Parsons, M. L., Walsh, W. J., Settlemier, C. J., White, D. J., Ballauer, J. M., Ayotte, P. M., . . . Carman, B. (2008). A multivariate assessment of the coral ecosystem health of two embayments on the lee of the island of Hawaiʻi. *Marine Pollution Bulletin*, *56* (6), 1138–1149. https://doi.org/10.1016/j.marpolbul.2008.03.004

Perry, C. T., Murphy, G. N., Kench, P. S., Edinger, E. N., Smithers, S. G., Steneck, R. S., & Mumby, P. J. (2014). Changing dynamics of Caribbean reef carbonate budgets: Emergence of reef bioeroders as critical controls on present and future reef growth potential. *The Royal Society*, *281*. https://doi.org/10.1098/rspb.2014.2018

Perry, C. T., Murphy, G. N., Kench, P. S., Smithers, S. G., Edinger, E. N., Steneck, R. S., & Mumby, P. J. (2013). Caribbean-wide decline in carbonate production threatens coral reef growth. *Nature Communications*, *4*, 1402. https://doi.org/10.1038/ncomms2409

Peterson, R. N., Burnett, W. C., Glenn, C. R., & Johnson, A. G. (2009). Quantification of point-source groundwater discharges from the shoreline of the Big Island, Hawaii. *Limnology and Oceanography: Methods*, *54*, 890–904. https://doi.org/10.4319/lo.2009.54.3.0890

Pierrot, D., Lewis, E., & Wallace, D. W. R. (2006). *MS Excel program developed for CO2 system calculations* (ORNL/CDIAC-105a). Oak Ridge, TN: Carbon Dioxide Information Analysis Center, Oak Ridge National Laboratory, U.S. Department of Energy.

Prouty, N. G., Yates, K. K., Smiley, N. A., & Gallagher, C. (2017). *Coral growth parameters and seawater chemistry*, Kahekili, West Maui: U.S. Geological Survey data release. https://doi.org/10.5066/F7X34VPV

Reaka-Kudla, M. L. (1987). The global biodiversity of coral reefs: A comparison with rainforests. In M. L. Reaka-Kudla, D. E. Wilson, & E. O. Wilson (Eds.), *Biodiversity II: Understanding and protecting our natural resources* (pp. 83–108). Washington, DC: Joseph Henry/National Academy Press.

Redding, J. E., Myers-Miller, R. L., Baker, D. M., Fogel, M., Raymundo, L. J., & Kim, K. (2013). Link between sewage-derived nitrogen pollution and coral disease severity in Guam. *Marine Pollution Bulletin*, *73*(1), 57–63. https://doi.org/10.1016/j.marpolbul.2013.06.002

Rodgers, KuS., Jokiel, P. L., Brown, E. K., Hau, S., & Sparks, R. (2015). Over a decade of change in spatial and temporal dynamics of Hawaiian coral reef communities 1. *Pacific Science*, *69*(1), 1–13. https://doi.org/doi:10.2984/69.1.1

Ross, M., White, D., Aiwohi, M., Walton, M., Sudek, M., Lager, D., & Jokiel, P. (2012). Characterization of "dead zones" and population demography of Porites compressa along a gradient of anthropogenic nutrient input at Kahekili Beach Park, Maui (Final Rep. for Project C11722). Honolulu, HI: State of Hawaii, Department of Land and Natural Resources, Division of Aquatic Resources.

Ryabenko, E., Altabet, M. A., & Wallace, D. W. R. (2009). Effect of chloride on the chemical conversion of nitrate to nitrous oxide for δ15N analysis. *Limnology and Oceanography: Methods*, *7*, 545–552. https://doi.org/10.4319/lom.2009.7.545

Sammarco, P. W., Risk, M. J., & Rose, C. (1987). Effects of grazing and damselfish territoriality on internal bioerosion of dead corals: Indirect effects. *Journal of Experimental Marine Biology and Ecology*, *112*(2), 185–199. https://doi.org/10.1016/0022-0981(87)90116-X

Schönberg, C. H., Fang, J. K., Carreiro-Silva, M., Tribollet, A., & Wisshak, M. (2017). Bioerosion: The other ocean acidification problem: Contribution to the Themed Issue: 'Ocean Acidification. *ICES Journal of Marine Science*, *74*(4), 895–925. https://doi.org/10.1093/icesjms/fsw254

Scoffin, T. P., Stearn, C. W., Boucher, D., Frydl, P., Hawkins, C., Hunter, I. G., & MacGeachy, J. K. (1980). Calcium carbonate budget of a fringing reef on the west coast of Barbados: Part II—Erosion, sediments and internal structure. *Bulletin of Marine Science*, *30*, 475–508.

Scott, P. J. B., & Risk, M. J. (1988). The effect of Lithophaga (Bivalvia: Mytilidae) boreholes on the strength of the coral Porites lobata. *Coral Reefs*, *7*(3), 145–151.

Shamberger, K. E. F., Cohen, A. L., Golbuu, Y., McCorkle, D. C., Lentz, S. J., & Barkley, H. C. (2014). Diverse coral communities in naturally acidified waters of a Western Pacific reef. *Geophysical Research Letters*, *41*, 499–504. https://doi.org/10.1002/2013GL058489

Shamberger, K. E. F., Feely, R. A., Sabine, C. L., Atkinson, M. J., DeCarlo, E. H., Mackenzie, F. T., . . . Butterfield, D. A. (2011). Calcification and organic production on a Hawaiian coral reef. *Marine Chemistry*, *127*(1), 64–75.

Shaw, E. C., McNeil, B. I., & Tilbrook, B. (2012). Impacts of ocean acidification in naturally variable coral reef flat ecosystems. *Journal of Geophysical Research: Oceans*, *117*, C03038. https://doi.org/10.1029/2011JC007655

Sigman, D. M., Casciotti, K. L., Andreani, M., Barford, C., Galanter, M., & Bohlke, J. K. (2001). A bacterial method for the nitrogen isotopic analysis of nitrate in seawater and freshwater. *Analytical Chemistry*, *73*, 4145–4415. https://doi.org/10.1021/ac010088e

Silbiger, N. J., Donahue, M. J., & Brainard, R. E. (2017). Environmental drivers of coral reef carbonate production and bioerosion: A multi-scale analysis. *Ecology*, *98*, 2547–2560. https://doi.org/10.1002/ecy.1946

Silbiger, N. J., Guadayol, Ò., Thomas, F. I. M., & Donahue, M. J. (2014). Reefs shift from net accretion to net erosion along a natural environmental gradient. *Marine Ecology Progress Series*, *515*, 33–44.

Silbiger, N. J., Guadayol, Ò., Thomas, F. I. M., & Donahue, M. J. (2016). A Novel μCT analysis reveals different responses of bioerosion and secondary accretion to environmental Variability. *PLoS ONE*, *11* (4), e0153058. https://doi.org/10.1371/journal.pone.0153058

Smith, J. E., Runcie, J. W., & Smith, C. M. (2005). Characterization of a large-scale ephemeral bloom of the green alga *Cladophora sericea* on the coral reefs of West Maui, Hawaii. *Marine Ecology Progress Series*, *302*, 77–91.

Sparks, R. T., Stone, K., White, D. J., Ross, M., & Williams, I. D. (2016). *Maui and Lanai monitoring report*. Wailuku, HI: Hawaii Department of Land and Natural Resources, Division of Aquatic Resources.

Stearn, C. W., Scoffin, T. P., & Martindale, W. (1977). Calcium carbonate budget of a fringing reef on the west coast of Barbado. Part I—Zonation and productivity. *Bulletin of Marine Science*, *27*, 479–510.

Swarzenski, P. W., Dulai, H., Kroeger, K., Smith, C., Dimova, N., Storlazzi, C., . . . Glenn, C. (2016). Observations of nearshore groundwater discharge: Kahekili Beach Park submarine springs, Maui, Hawaii. *Journal of Hydrology: Regional Studies*, *11*, 147–165, https://doi.org/10.1016/j.ejrh.2015.12.056

Swarzenski, P. W., Storlazzi, C. D., Presto, M. K., Gibbs, A. E., Smith, C. G., Dimova, N. T., . . . Logan, J. B. (2012). Nearshore morphology, benthic structure, hydrodynamics, and coastal groundwater discharge near Kahekili Beach Park, Maui, Hawaii (U.S. Geol. Surv. Open-File Rep. 2012-1166, 34 p.). Reston, VA: U.S. Geological Survey.

Tribollet, A., Godinot, C., Atkinson, M., & Langdon, C. (2009). Effects of elevated pCO_2 on dissolution of coral carbonates by microbial euendoliths. *Global Biogeochemical Cycles*, *23*, GB3008. https://doi.org/10.1029/2008GB003286

Tribollet, A., & Golubic S. (2011). Reef bioerosion: Agents and processes. In Z. Dubinsky & N. Stambler (Eds.), *Coral reefs: An ecosystem in transition* (pp. 435–449). Dordrecht, the Netherlands: Springer.

Tunnicliffe, V. (1979). The role of boring sponges in coral fracture. *Biologie Des Spongiaires*, *291*, 309–315.

Tunnicliffe, V. (1981). Breakage and propagation of the stony coral Acropora cervicornis. *Proceedings of the National Academy of Sciences United States of America*, *78*(4), 2427–2431.

van Hooidonk, R., Maynard, J. A., Manzello, D., & Planes, S. (2014). Opposite latitudinal gradients in projected ocean acidification and bleaching impacts on coral reefs. *Global Change Biology*, *20*(1), 103–112. https://doi.org/10.1111/gcb.12394

Vega Thurber, R. L., Burkepile, D. E., Fuchs, C., Shantz, A. A., McMinds, R., & Zaneveld, J. R. (2014). Chronic nutrient enrichment increases prevalence and severity of coral disease and bleaching. *Global Change Biology*, *20*(2), 544–554. https://doi.org/10.1111/gcb.12450

Wang, G., Jing, W., Wang, S., Xu, Y., Wang, Z., Zhang, Z., . . . Dai, M. (2014). Coastal acidification induced by tidal-driven submarine groundwater discharge in a coastal coral reef system. *Environmental Science & Technology*, *48*(22), 13069–13075. https://doi.org/10.1021/es5026867

Wang, Z. A., & Cai, W.-J. (2004). Carbon dioxide degassing and inorganic carbon export from a marsh-dominated estuary (the Duplin River): A marsh CO_2 pump. *Limnology and Oceanography: Methods*, *49*(2), 341–354. https://doi.org/10.4319/lo.2004.49.2.0341

Wiedenmann, J., D'angelo, C., Smith, E. G., Hunt, A. N., Legiret, F.-E., Postle, A. D., & Achterberg, E. P. (2013). Nutrient enrichment can increase the susceptibility of reef corals to bleaching. *Nature Climate Change, 3* (2), 160–164. https://doi.org/10.1038/nclimate1661

Williams, I. D., White, D. J., Sparks, R. T., Lino, K. C., Zamzow, J. P., Kelly, E. L. A., & Ramey, H. L. (2016). Responses of herbivorous fishes and benthos to 6 years of protection at the Kahekili Herbivore fisheries management area, Maui. *PLoS ONE*, *11* (7), e0159100. https://doi.org/10.1371/journal.pone.0159100

Wiltse, W. (1996). *Algal blooms: Progress report on scientific research* (64 pp.). Honolulu, HI: West Maui Watershed Management Project, State of Hawaii Department of Health.

Yao, W., & Byrne, R. H. (1998). Simplified seawater alkalinity analysis: Use of linear array spectrometers. *Deep Sea Research Part I: Oceanographic Research Papers*, *45*(8), 1383–1392.

Yates, K. K., Zawada, D. G., Smiley, N. A., & Tiling-Range, G. (2017). Divergence of seafloor elevation and sea level rise in coral reef ecosystems. *Biogeosciences*, *14*(6), 1739–1772. https://doi.org/10.5194/bg-14-1739-2017

Zhang, H., & Byrne, R. H. (1996). Spectrophotometric pH measurements of surface seawater at in-situ conditions: Absorbance and protonation behavior of thymol blue. *Marine Chemistry*, *52*(1), 17–25. https://doi.org/10.1016/0304-4203(95)00076-3